

Experimental Study on Post-Earthquake Fire Resistance of Ductile Concrete-Filled Double-Skin Tube Columns

R. Imani, S.M.ASCE¹; G. Mosqueda, A.M.ASCE²; and M. Bruneau, F.ASCE³

Abstract: Experimental studies were conducted to examine the behavior of concrete-filled double-skin tube (CFDST) columns exposed to fire after being subjected to simulated seismic loads. The experiments were conducted in two separate phases, consisting of (1) the quasi-static cyclic tests, followed by (2) fire tests. Three nominally identical column specimens were constructed for these studies. One of the specimens was directly tested under fire to quantify its resistance in an undamaged condition. The other two specimens were first subjected to quasi-static cyclic lateral loads, imposing varying degrees of lateral drift to simulate two different seismic events with moderate and high damage levels before being exposed to fire. Both of the specimens were pushed to the maximum drift of 6–6.5% with different residual drifts of 1.4 and 3.9% for moderate and high damage levels, respectively. The undamaged and damaged columns were then subjected to the same fire tests in accordance with a standard temperature-time curve while sustaining an axial load until the column failed due to global buckling. Local buckling of the tubes was also observed in the specimens due to the thermal expansion and separation from the concrete. Overall the results showed marginal differences in the fire resistance of the three specimens, providing evidence for the resilient performance of these columns under post-earthquake fire scenarios. An additional quasi-static cyclic loading test was conducted on the specimen that had been exposed to fire without any prior damage to investigate the behavior of the column subjected to seismic loads after the fire test. Differences in behavior were modest, except for a 5.7% drop in strength attributed to permanent degradation in material properties due to the fire test. DOI: [10.1061/\(ASCE\)ST.1943-541X.0001168](https://doi.org/10.1061/(ASCE)ST.1943-541X.0001168). © 2014 American Society of Civil Engineers.

Author keywords: Fire following earthquake; Concrete-filled double-skin tube columns; Composite columns; Multihazard design; Seismic performance; Cyclic testing; Fire resistance; Post-earthquake fire resistance.

Introduction

The 1906 San Francisco and the 1923 Tokyo earthquakes caused severe damage due to the ground shaking; however, damage and losses from the subsequent fires reportedly exceeded damage from the shaking itself (NOAA 1972). At a smaller scale hundreds of fires were reported after the 1989 Loma Prieta, 1994 Northridge, and 1995 Kobe earthquakes. Although no widespread conflagrations occurred after these earthquakes, in Kobe alone almost 7,000 buildings were damaged by fire (NIST 1996). Considering the risk of fire either locally within buildings or conflagrations after an earthquake, the effects of seismic damage on the fire resistance of structural members need to be better understood for resilient structural design.

Concrete-filled steel tubes (CFSTs) are a promising multihazard resistant structural system exhibiting high performance for different types of extreme events. More recently, ductile concrete-filled double-skin tube (CFDST) columns have also been investigated under both seismic and blast loadings and provided good performance under these different loading conditions (Fouché and Bruneau

2010). Past studies have demonstrated the desirable seismic performance of CFSTs (Hajjar 2000; Marson and Bruneau 2004; Han and Yang 2005) and CFDSTs (Zhao and Grzebieta 2002; Han et al. 2004; Uenaka et al. 2008), while separate studies have addressed the fire resistance of CFSTs (Kodur 1998; Han 2001, 2003; Hong and Varma 2009; Moliner et al. 2013) as well as CFDSTs (Yang and Han 2008; Lu et al. 2010).

Lu et al. (2010, 2011) showed through both experimental and numerical studies that CFDST columns can have better fire endurance than CFST columns due to the structural contribution of the inner tube that benefits from the fire protection provided by the concrete. Compared to CFST columns, CFDST columns also have larger stiffness-to-weight and strength-to-weight ratios (due to the material being distributed farther from the center of the cross section), which is also advantageous for lateral load resistance.

This paper expands on these previous studies by investigating the behavior of CFDSTs when exposed to fire after an earthquake. More specifically, the behavior of such columns under fire is examined after being subjected to various levels of damage from simulated earthquake loading. In addition, to a limited degree, the effect of fire on the seismic capacity of structural column is also investigated. This paper describes the seismic and fire experiments that were carried out to assess the behavior of CFDST columns.

Experimental Program

An experimental study was conducted to investigate the behavior of CFDST columns subjected to fire after earthquake loading. Three nominally identical column specimens were subjected to a fire test. Two of those three columns had first been subjected to cyclic inelastic loading to simulate different levels of seismic damage and residual deformations; the other column, beyond serving as the

¹Graduate Research Assistant, Dept. of Civil, Structural, and Environmental Engineering, Univ. at Buffalo, Buffalo, NY 14260 (corresponding author). E-mail: rezaiman@buffalo.edu

²Associate Professor, Dept. of Structural Engineering, Univ. of California at San Diego, La Jolla, CA 92093. E-mail: gmosqueda@ucsd.edu

³Professor, Dept. of Civil, Structural, and Environmental Engineering, Univ. at Buffalo, Buffalo, NY 14260. E-mail: bruneau@buffalo.edu

Note. This manuscript was submitted on February 6, 2014; approved on August 6, 2014; published online on September 8, 2014. Discussion period open until February 8, 2015; separate discussions must be submitted for individual papers. This paper is part of the *Journal of Structural Engineering*, © ASCE, ISSN 0733-9445/04014192(10)/\$25.00.

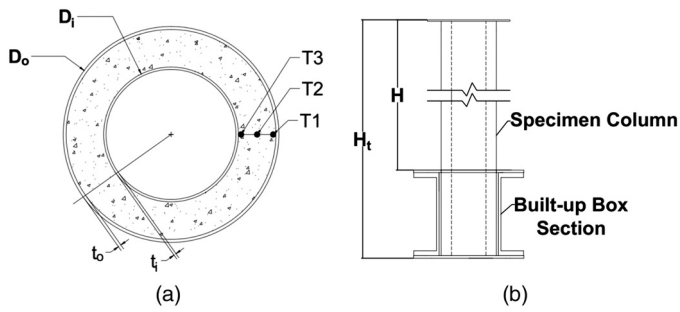


Fig. 1. Schematic of specimen: (a) cross section with thermocouple layout; (b) elevation (specimen with the additional built-up box)

reference specimen against which to compare the fire performance of the other two columns, was subjected to cyclic testing after its fire test to investigate the reversed problem of earthquake after fire. The details of the specimens and experimental setups for seismic and fire testing are described in the subsequent sections. The seismic tests were conducted at the Structural Engineering and Earthquake Simulation Laboratory (SEESL), University at Buffalo, and the fire tests were conducted using a furnace at NGC Testing Services in Buffalo, New York.

Specimens

The specimens used in the research reported in this paper were selected from a set of quarter-scale CFDST columns tested by Fouché and Bruneau (2010) in multihazard (earthquake and blast) conditions, and modified to comply with the limitations of the cyclic and fire test setups. The three specimens were designed and constructed with the geometric properties shown [Figs. 1(a and b)], and Table 1 lists the dimensions. Both inner and outer tubes satisfy the ductility requirements of AISC (2010), with diameter-to-thickness (D_o/t_o and D_i/t_i) ratios of 55.6 (highly ductile) and 72.2 (moderately ductile), where D_o and D_i are the diameters of the outside and inside tube, respectively; and t_o and t_i are thickness for the same.

Specimens were constructed of ASTM A513 Type 1 (ASTM 2012a) steel tubes with nominal yield and tensile strength of 220 and 310 MPa (32 and 45 ksi), respectively (coupon tests resulted in average yield and tensile strength values of 325 and 380 MPa, respectively). Cylinder tests from the self-compacting concrete used for the specimens (conducted on the test dates) showed an average compressive stress of 61 MPa (8.8 ksi).

Due to the construction sequence both the inner and outer tubes were welded to column base plates, while only the outer tube was welded to the cap plate at the top end. In addition to the three column specimens, three stub columns were also fabricated to be used in the fire tests to collect additional data on the heat transfer process to the inner tube. The stub columns had cross sections identical to the column specimens, but they only had a length of 304.8 mm (12 in.).

Table 1. Geometric Properties of the Tested Columns

Column type	Height, H [mm (in.)]	Diameter of outer tube, D_o [mm (in.)]	Diameter of inner tube, D_i [mm (in.)]	Thickness of outer tube, t_o [mm (in.)]	Thickness of inner tube, t_i [mm (in.)]	Ductility class	
						Inner tube	Outer tube
Specimen	2,705.1 (106.5)	203.2 (8)	127.0 (5)	2.79 (0.11)	2.29 (0.09)	MD	HD
Stub	304.8 (12)	203.2 (8)	127.0 (5)	2.79 (0.11)	2.29 (0.09)	MD	HD

Note: HD = highly ductile; MD = moderately ductile.

Test Setup for Cyclic Loading

Fig. 2(a) shows the experimental setup for seismic loading. The column specimens were fixed at their base on a lateral foundation beam to form a vertical cantilever condition. Boundaries of specimen columns consisted of a cap plate on the top end, connected to a 220-kN (50-kip) actuator using a load transfer element. A constant axial load was applied using a post-tensioned threaded rod running through the void in the middle of the specimen [Fig. 2(a)]. The tensile load in the post-tensioned rod was monitored using a load cell throughout the cyclic loading tests and showed an average change of about $\pm(2.0 - 2.5\%)$, including the increases at peak drifts and the decrease at the end of the tests. The flexural strength of the bottom end was substantially increased in the loading direction, using two channels on the sides of the column and plates at the top and bottom of the channels, to force plastic hinging to develop at the top of the resulting built-up box [Fig. 1(b)].

The bottom end of the specimen was tied to the base beam using pretensioned rods running through the channels on both sides. Tube stubs were inserted between top and bottom flanges of channels to prevent undesirable flange deflections. Two of the specimens (S1 and S2) were tested under cyclic lateral loading, keeping the third specimen (S3) undamaged for the fire test. Two sets of displacement recording devices [i.e., (1) string pots, and (2) a Krypton dynamic measurement system] and a set of strain gauges were used to record the distribution of displacements and strains in different parts of the columns. Load cells were used to monitor both the axial and lateral loads applied to the column specimen.

Cyclic Testing Procedure

Axial load level was planned to be about 30% of the nominal axial strength of the specimens calculated using the measured material properties (typical load level for columns in a building). However, due to technical difficulties in getting to that load level for the post-tensioning bar, the applied force was limited to 311 kN (70 kips) for specimen S1 and, after a slight enhancement of the loading system, 356 kN (80 kips) for specimen S2 (which are about 19 and 21% of the axial load capacity, respectively). Specimens S1 and S2 were tested in displacement controlled mode using the cyclic load protocol recommended in ATC-24 [ATC 1992; Fig. 2(b)]. The cyclic displacement amplitude was increased up to the point where the desired damage level for the specimen could be visually identified. The first specimen (S1) was subjected to cyclic displacements until the first visual signs of local buckling appeared on the outer tube after attainment of its plastic moment. This level was considered a moderate damage state resulting from a moderate inelastic history for the specimen. The second specimen (S2) was pushed further (i.e., subjected to additional cycles) to reach a higher damage level but testing stopped before any fracture developed. Significant reduction in the specimen's lateral resisting force (about 10–20%) was used as test termination criteria. Residual drift was used as an indicator to distinguish between the damage levels of the two specimens.

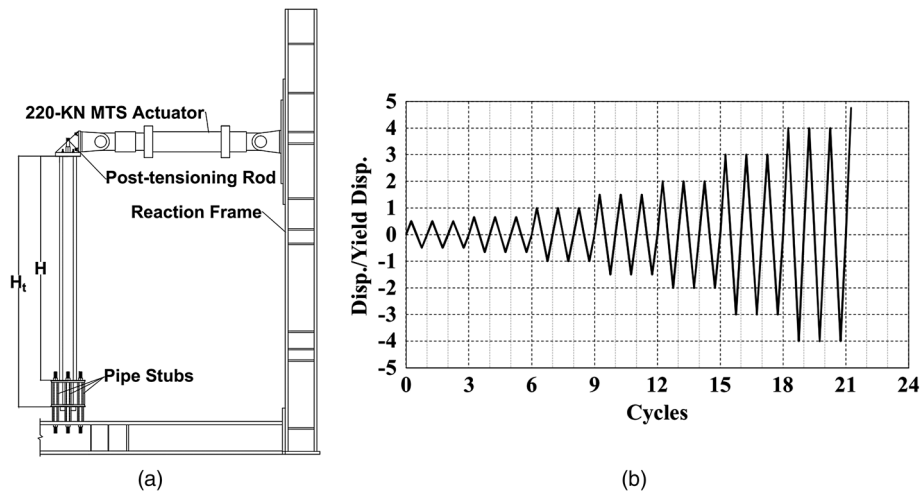


Fig. 2. Cyclic testing of specimens: (a) test setup; (b) protocol for displacement controlled cyclic testing

Fire Testing Setup

The height of the columns examined in the research reported in this paper was limited by the 3048-mm (120-in.) vertical clearance of the furnace available at NGC Testing Services. Boundaries of the furnace were defined by two concrete beams at the top and bottom, framing between two concrete columns, a moving wall on one side of the plane delimited by these beams and columns, and a fixed wall on the other side of the furnace. The top and bottom beams were 406.4- and 304.8-mm (16- and 12-in.) wide, respectively. The top beam was fixed in place, working as a reacting member to vertical loads applied to it by the top of the column specimen (in compression). The bottom beam was attached to a railing that

allowed vertical movement over a total travel distance of 101.6 mm (4 in.) [± 50.8 mm (± 2 in.)]. The beam was supported from below by eight hydraulic actuators that were used to apply vertical compression loads to the tested specimens (and evenly distributed to prevent bottom beam rotation, although slight rotations could be accommodated by the system due to minor actuator misalignments). The maximum load was limited to 534 kN (120 kips) [i.e., 67 kN (1 kip) per actuator]. Fig. 3(a) shows a photo of the vertical furnace, with the specimen between the top and bottom beams. Fig. 3(b) shows a drawing of the fire test setup. A photo of the hydraulic actuators below the bottom beam is shown [Fig. 3(c)].

The three specimens were prepared for the fire tests with a few modifications at both ends to comply with the boundaries of the

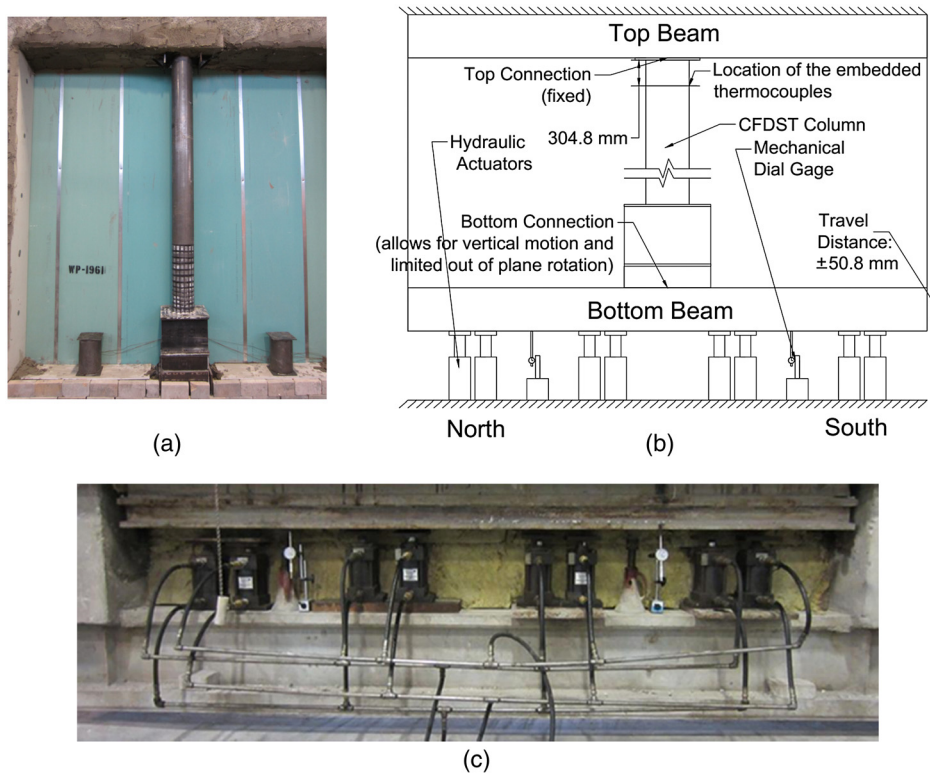


Fig. 3. Fire test setup: (a) Specimen S1 in the vertical furnace with two stub columns (SC1 and SC2); (b) schematic of the fire test setup; (c) hydraulic actuators below the bottom beam

vertical furnace. Two sets of thermocouples were used to record the temperature distribution response around and within the specimens, i.e., (1) a group of nine thermocouples was installed in different parts of the furnace and used to control the furnace air temperature, and (2) a group of three thermocouples embedded in concrete was used to record the temperature distribution within the column [two were installed on the surfaces of the inner and outer tubes, with the third one in the middle of the concrete region per Fig. 1(a)].

The embedded thermocouples were installed near the top end of the specimens about 304.8 mm (12 in.) from the top plate [Fig. 3(b)]. This location was chosen due to its ease of access during construction. The variation of temperature along the height of the column can be studied by monitoring the temperature values from the furnace thermocouples (the set of nine mentioned previously), which record the furnace air temperature at different locations. The wires attached to these thermocouples were led out of the specimens through one of the four small diameter (1/4 in.) vent holes, which were drilled on the outer tube to provide escape routes for the pressurized vapor during the fire tests (two holes at each end of the column). The number and locations of the vent holes were determined based on AISC (2003) design guide for fire resistance of structural steel framing. The same set of three thermocouples was installed on the stub columns. The number of vent holes for the stub columns were reduced to two (one at each end) because of their much shorter length, except for Stub Column SC2 that was fabricated with three holes in an attempt to study the effects of the number of vent holes on the heat transfer process in columns.

Fire Testing Procedure

The constant axial load applied to specimens during the tests was controlled by maintaining the equivalent pressure needed for the

hydraulic pumps to exert the load up to the desired level. Axial displacement of the columns was measured according to the movements of the bottom beam by manual readings of two mechanical gauges at intervals during the tests. The gauges were placed under the bottom beam at two sides and had an accuracy of 0.025 mm (0.001 in.).

Fire tests were in accordance with the ASTM E119 (ASTM 2012b) curve. The tests were continued until the column could no longer resist the axial load. This failure criterion could be confirmed by observation of global buckling of the specimen or by detecting an increased velocity [close to 25 mm/min (1 in./min)] in the vertical movement of the bottom beam supporting the specimen, indicating that the column was shortening under the axial load. Specimen S3 (the undamaged column) was selected for the first fire test, and next were Specimens S1 and S2. Two of the three stub columns (SC1 and SC2), built to be used as additional references for temperature distribution analyses, were tested in the same furnace with Specimen S1. Stub Column SC3 was not subjected to the fire tests for subsequent use as a reference model.

Test Results and Discussion

A complete list of the experiments conducted in this study is presented (Table 2). Major results and observations are summarized in the subsequent sections.

Cyclic Testing of Specimens S1 and S2

Fig. 4 shows the resulting lateral force versus lateral drift curves recorded for Specimens S1 and S2. These lateral drift values were calculated by correcting the recorded displacements to eliminate

Table 2. Summary of the Experimental Program

Test type	Specimen	Axial load [kN (kip)]	Maximum drift (%)	Residual drift (%)	Simulated seismic damage level	Fire resistance time (min)
Cyclic loading tests	S1	311 (70)	6.2	1.4	Moderate	N/A
	S2	356 (80)	6.3	3.9	High	N/A
	S3	N/A	N/A	N/A	None	N/A
Fire tests per ASTM E119 (ASTM 2012b)	S3	311 (70)	N/A	N/A	None	65
	S1	311 (70)	N/A	N/A	Moderate	65
Post-fire cyclic loading test	S2	356 (80)	N/A	N/A	High	60
	S3 (after 65-min fire)	0	11	0.05 (test terminated after a 50% strength loss)	Specimen fractured	N/A

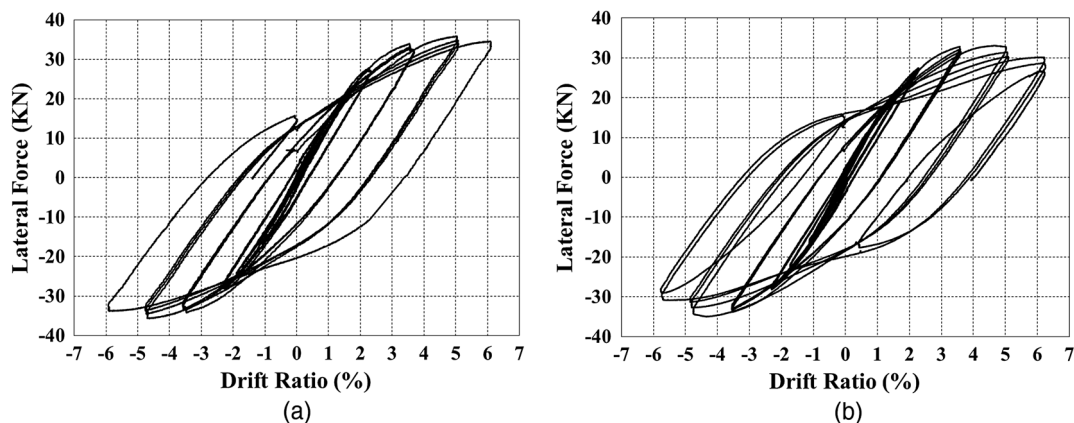


Fig. 4. Lateral force versus drift ratio results of cyclic testing: (a) Specimen S1; (b) Specimen S2

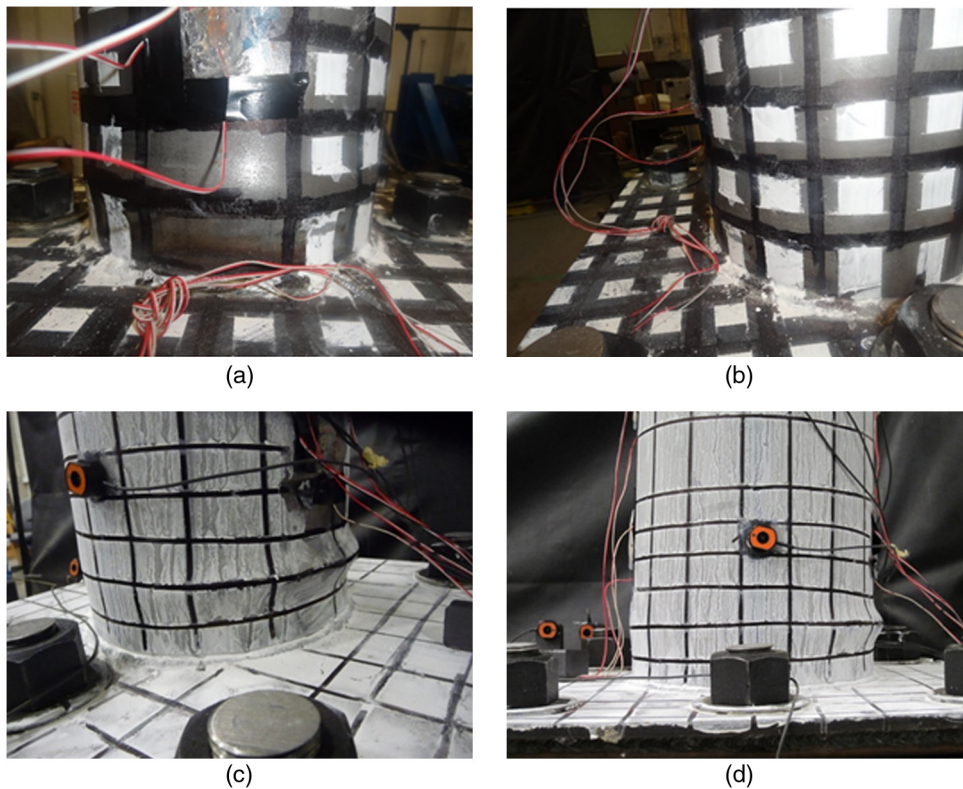


Fig. 5. Local buckling of the outer steel tube at the base of the columns: (a) Specimen S1 (first view); (b) Specimen S1 (second view); (c) Specimen S2 (first view); (d) Specimen S2 (second view)

the small contribution resulting from base flexibility. Results show that Specimen S1 did not lose significant strength until the last cycle of loading, when a strength degradation of approximately 5% occurred. This degradation is expected as it occurred during the only cycle for which local buckling could be seen to develop at the base of the outer tube. The maximum lateral drift of Specimen S2 was similar to that of Specimen S1, but additional inelastic cycles were applied to Specimen S2 to increase damage that resulted in a larger residual drift compared to Specimen S1 when unloaded.

Fig. 5 shows local buckling of the outer steel tube at the base of both specimens. Specimen S2 suffered more severe buckling as indicated by the level of bulging of the steel due to the additional loading cycles. This is in agreement with the lateral force versus lateral drift graphs (Fig. 4), which shows a higher amount of strength degradation for Specimen S2 (about 20% for the final half cycle of loading). Cyclic tests ended with maximum and residual drift ratios of 6.2 and 1.4% for Specimen S1 (moderate damage level), and 6.3 and 3.9% for Specimen S2 (high damage level), respectively. The tested columns, along with Specimen S3 (with no simulated seismic damage), were then subjected to the fire test described in the subsequent section.

Fire Test 1, Specimen S3

Specimen S3 was exposed to an ASTM E119 (ASTM 2012b) fire, under an axial load of 311 kN (70 kips) (the same amount that was used in the cyclic tests). Fig. 6(a) shows the history of the average furnace temperature along with the temperature data recorded by the thermocouples embedded in the specimen. The average furnace temperature closely matches the ASTM E119 (ASTM 2012b) curve, as intended. Looking into individual recordings from the furnace

temperatures showed a maximum difference of about 100°C between them (lower parts of the furnace had slightly lower temperatures), which was about 10% of the maximum reached temperature value for the test (approximately 970°C). It was inferred that the column was exposed to almost uniform temperatures along its height. The difference between the temperature of the inner and outer tubes throughout the test shows the effectiveness of the concrete in insulating the inner tube. It is speculated that the sudden fluctuations in the recorded temperature data can be related to water content of the concrete traveling within the specimen and creating corresponding pressure changes (as a result of vaporization of the moisture content of the concrete during the fire test, which builds up pressure between the inner and outer tubes, as well as throughout the concrete core). These fluctuations appeared to be temporary, allowing the temperature curves to follow the expected trend after a while.

The fire resistance time was recorded to be about 65 min for Specimen S3. Fig. 7(a) shows the axial displacement of the column as measured by the movement of the bottom beam during the test. Two curves are plotted based on the data from the mechanical gauges placed on the north and south sides of the beam. Small rotations of the beam developed during the test due to slight unavoidable misalignment of the loads. Since the north and south gauges differed, the average of the two readings was considered as the axial displacement for the column in Fig. 7(a). The recorded travel distance from both of the gauges was in the range of ± 0.5 in., which is less than the travel distance limit of ± 2 in., that could be accommodated by the bottom (moving) beam (hence, no axial constraints were imposed against thermal expansion in addition to the applied axial load).

As indicated [Fig. 7(a)], the specimen goes through four stages during the fire test. These are similar to the four stages of the mechanical behavior of conventional concrete-filled tube columns

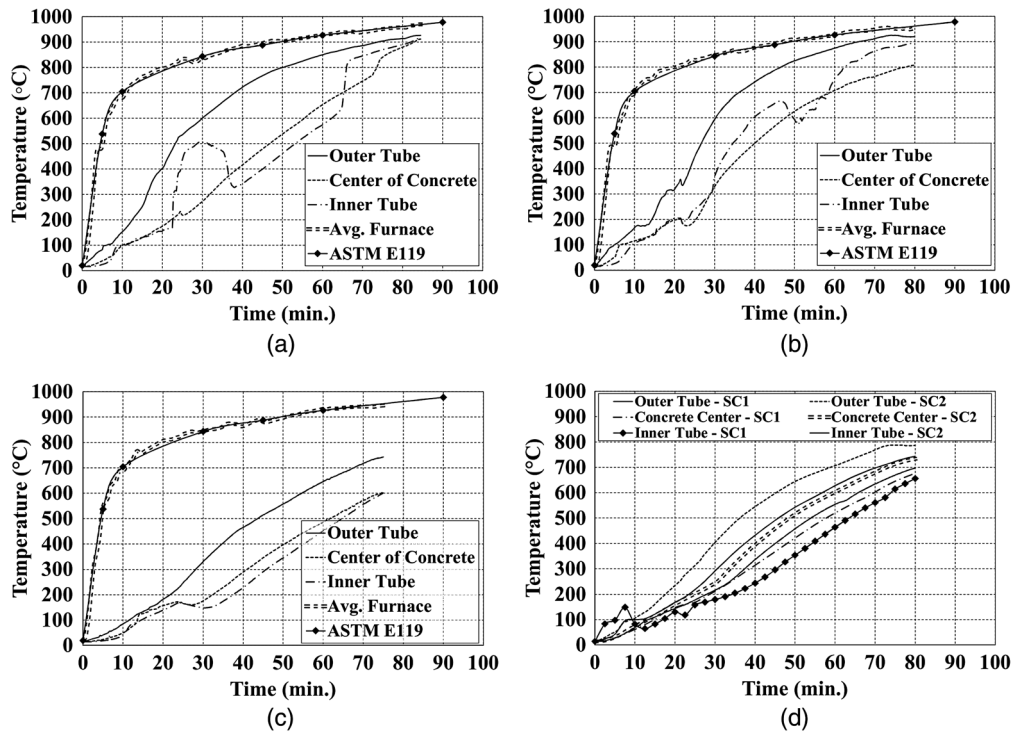


Fig. 6. ASTM E119 (ASTM 2012b) fire curve along with the temperature distribution results measured in fire tests: (a) Specimen S3; (b) Specimen S1; (c) Specimen S2; (d) SC1 and SC2

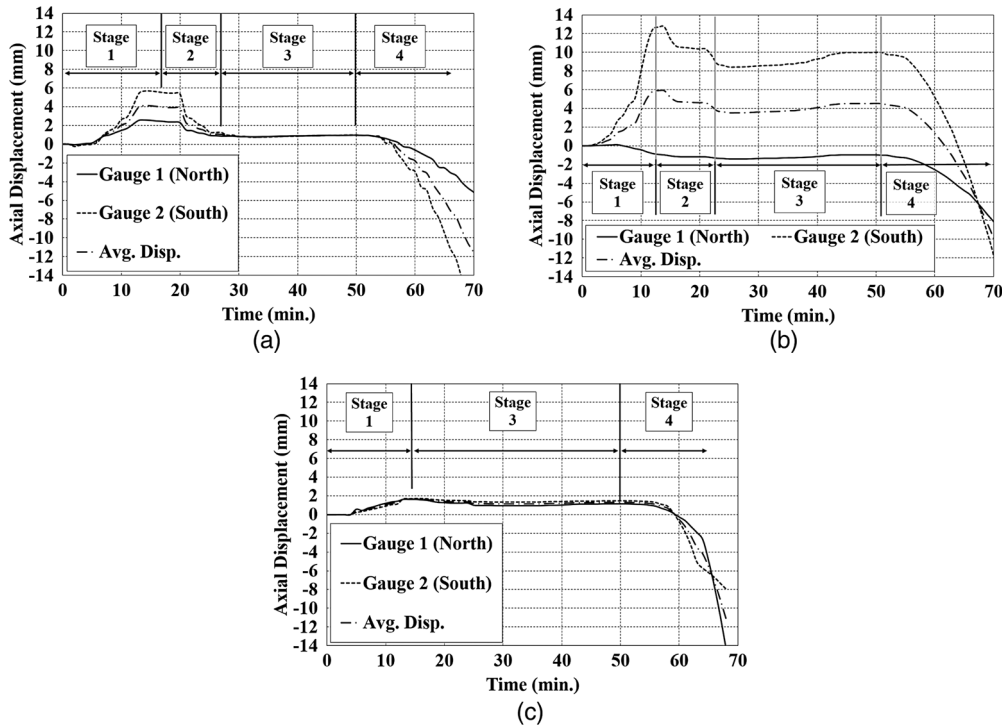


Fig. 7. Axial displacement results from fire tests: (a) Specimen S3; (b) Specimen S1; (c) Specimen S2

presented in a numerical study by Espinos et al. (2010). The first stage lasts about 12 min and consists of an expansion process in which the outer steel tube expands faster than the concrete core and inner tube. As a result the outer steel tube carries the entire axial load. The second stage occurs a few minutes later when

the outer tube reaches higher temperatures, weakening the steel, and can no longer sustain the load. This stage is accelerated by local buckling of the outer tube under the 311-kN (70-kip) load, creating the sudden drop in the axial displacement plots, which continues until the concrete is engaged anew in carrying the axial load.

The third stage starts after the drop, when the tubes and the concrete are working together until about 55 min from the start of the test. During this period the specimen is either expanding slightly or just maintaining its length while resisting the axial load. The last stage starts when the specimen can no longer resist the axial load and the displacement begins to increase at a significantly higher rate. The test ends a few minutes later when global buckling is visually confirmed and the bottom beam is moving with a rate close to 25 mm/min (1 in./min).

Fig. 8(a) shows the local buckling of the outer tube of Specimen S3, close to the top beam of the furnace. Although the movement is occurring at the bottom beam, no local buckling or any other damage is seen around that location. Buckling in the outer tube occurs on the top end because the gap between the concrete and end plates is more likely to occur on the top end. As the outer tube is heated and thermally expands longitudinally and transversely at a faster rate compared to the concrete core, the two separate. The concrete remains on the bottom end due to its self-weight, forming a gap with the top end plate of the column and leaving the outer tube to support all of the applied axial load [311 kN (70 kips)] through the gap section.

The final state of the specimen just after the end of the test showed its failure with an out-of-plane global buckling mechanism [Fig. 8(b)]. The out-of-plane direction refers to the out-of-plane of the frame of the furnace [Fig. 3(b)]. The connection at the top [Fig. 3(b)] worked as a fixed connection, creating an inflection point in the upper part of the specimen. Observation of the bottom end of the specimen revealed that the out-of-plane rotation of this connection was not fully restrained (and functioned as a semirigid joint), thus allowing limited out of plane rotation for the bottom end of the specimen [Fig. 3(b)]. This limited rotation could have contributed to the direction of the global buckling in the out-of-plane

orientation. Another reason for a tendency to buckle out of plane was the fact that the specimen had more bending strength in the in-plane direction because of the greater in-plane fixity provided by the channels at the bottom.

Fire Test 2, Specimen S1

Specimen S1 with a residual drift of 1.4% after cyclic testing (considered as a moderate level of damage) was selected for the second fire test. The column was modified to fit within the boundaries of the vertical furnace in the same manner as Specimen S3. The only difference was that considering the lack of straightness of Specimen S1 due to its residual drift, built-up channels were welded to both ends of the column at a slightly inclined angle. This modification was needed to get two flat and parallel surfaces at the top and bottom of the specimen to properly sit within the furnace. Vertical alignment of the center points of the column's top and bottom plates was considered during installation to ensure the concentricity of the applied axial load. The damaged end of the column was positioned close to the bottom beam of the furnace. The specimen was subjected to an axial load of 311 kN (70 kips) and exposed to the ASTM E119 (ASTM 2012b) standard fire while the axial load was maintained. The test was terminated due to global buckling of the specimen, with a recorded fire resistance time of about 65 min. The resistance time showed that the seismic damage did not significantly affect the general performance of the column under fire loading.

Fig. 6(b) shows the data recorded by the thermocouples inside the furnace and within the specimen. The results are similar to the data reported from the first fire test as expected since the two specimens are nominally identical. This data also shows that the moderate seismic damage induced at the base of the column did not affect the heat transfer process in the specimen.

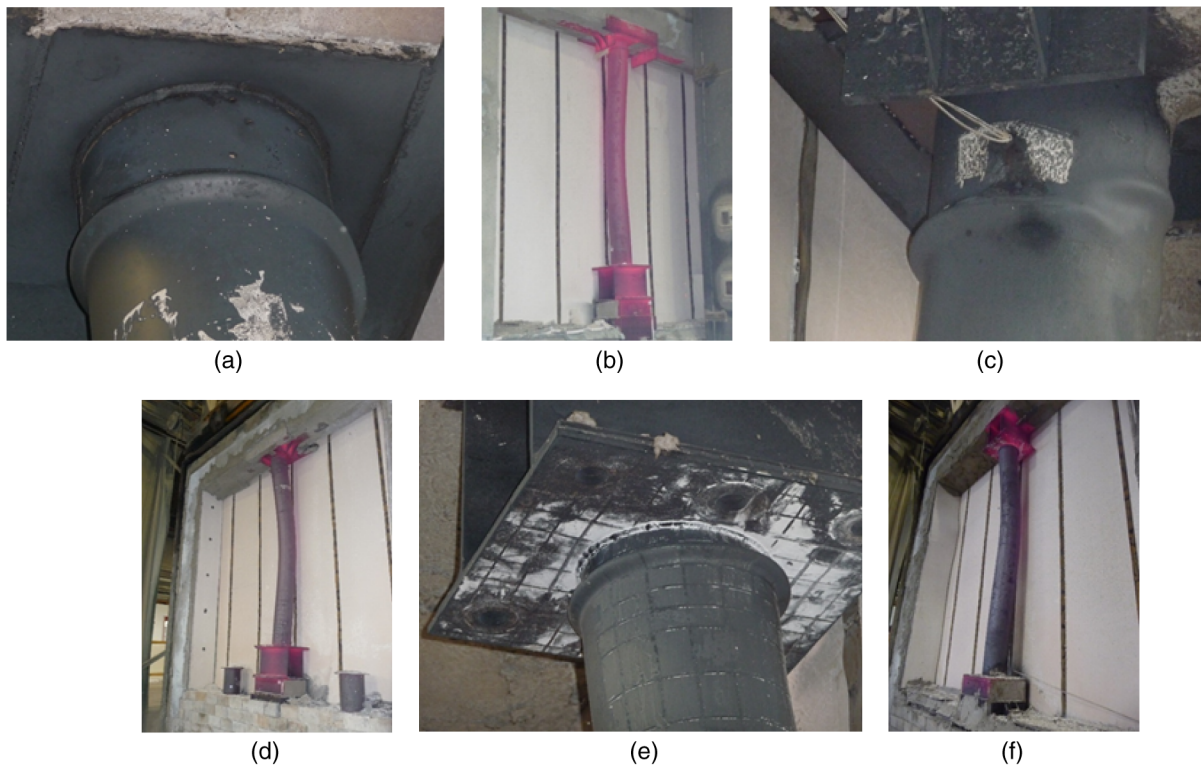


Fig. 8. Local and global buckling of specimen columns tested in fire: (a) Specimen S3 (local); (b) Specimen S3 (global); (c) Specimen S1 (local); (d) Specimen S1 (global); (e) Specimen S2 (local); (f) Specimen S2 (global)

The axial displacement history of the column went through the same four stages of behavior described for the previous test specimen [Fig. 7(b)]. Although initial damage was imposed at the bottom end of the outer tube from cyclic testing, local buckling during the fire test occurred at the top of the column, as in the previous test (for the same reasons described previously). Different locations of the seismic damage (at the bottom end of the column) and fire damage (local buckling of the outer tube at the top end) limited any reduction in capacity of the column under combined fire-seismic damage. The fact that global buckling still occurred in the out of plane direction, even though the in-plane moment resistance of the column was subjected to cyclic loading (resulting in some stiffness reduction), supports the idea that the bottom end connection allowed for a limited out of plane rotation facilitating the out-of-plane oriented buckling. Figs. 8(c and d) show the local and global buckling of Specimen S1.

Fire Test 3, Specimen S2

Specimen S2 was prepared for the third fire test, with a residual drift of 3.9% from the lateral cyclic loading (considered as a highly damaged column). Considering the results from the first two fire tests, the setup for the third fire test was modified in two specific ways in an attempt to better capture the effects of prior cyclic loading on the performance of the specimen under fire.

First, Specimen S2 was inverted such that the seismically damaged end was connected to the top beam of the furnace. Connecting the damaged end of the column to the bottom beam of the furnace would have been necessary to allow direct comparison between the results of Specimen S2 and the first two fire tests [i.e., (1) Specimen S3, and (2) Specimen S1]. However, since it was known by this time that the fire-induced local buckling would occur at the column end close to the top beam of the furnace (for the reasons mentioned previously), Specimen S2 was inverted (i.e., to connect the damaged end to the top beam) in an attempt to simulate a worst case scenario, where local buckling effects due to seismic loading and fire conditions could combine, possibly leading to a lower fire resistance time.

Second, the specimen was installed in the furnace such that it was rotated 90° about its longitudinal axis with respect to the previous two columns. This orientation was selected to ensure that the out-of-plane buckling of the specimen would occur in the same direction that had already been weakened during the cyclic test.

The axial load for Specimen S2 was increased to 356 kN (80 kips) to match the axial load applied in the cyclic test. Although the column was considerably damaged due to cyclic loading prior to the fire test and was installed as indicated previously to maximize the impact of the prior seismic damage, the fire resistance time remained about 60 min. Fig. 6(c) shows the time history of temperature changes recorded by the thermocouples installed both within and out of Specimen S2 in the furnace area. The recordings show a similar trend compared to the previous tests. The only difference is that the temperature values measured for Specimen S2 are about, on average, 150–200°C lower than the temperatures recorded from Specimens S1 and S3 at the same points in time. The average furnace air temperature on the other hand is the same for all of the specimens. The difference might be due to some unexpected changes in the heat transfer process, as suggested by a loud sustained hissing noise (similar to a pressure relief mechanism) heard about 25 min into the test, and that faded out after about 5 min. This was speculated to be related to vaporization of the water content of concrete and its attempt to escape from the steel case.

The time history of axial displacement measured by the mechanical gauges for Specimen S2 are plotted [Fig. 7(c)]. The

marginal difference between the two readings showed that the bottom beam of the furnace moved up uniformly along its length.

Apart from the fire resistance time, which is controlled by global buckling in these tests, a few differences were observed in the behavior of Specimen S2 in comparison with the previous tests. The average maximum axial displacement in the expansion period was measured to be about 1.8 mm (0.07 in.), which is about 30–40% of the measured values for the other two specimens [4.0–5.8 mm (0.16–0.23 in.)]. Stage 2 (expressed by a sudden drop in the axial displacement) did not occur for Specimen S2 because of its significantly lower axial displacement in the expansion period compared to Specimens S1 and S3.

Two factors may have contributed to this observed difference in behavior. The first is related to the specific orientation of Specimen S2 in the furnace. Similar to the previous tests, the expansion of the outer tube was followed by its local buckling close to the top beam of the furnace. Specimen S2 already had initial local buckling in that area acting as a substantial initial imperfection. Therefore, from the beginning of the test, expansion of the outer tube contributed to enlarge the existing local-buckling ring at that location, rather than contributing to axial elongation of the column. The second factor possibly contributing to the smaller expansion of Specimen S2 is based on the fact that Specimen S2 had lower temperature values compared to the other two specimens (maximum temperature for the outer tube of Specimen S2 was about 720°C as opposed to 920°C for Specimens S1 and S3). Lower temperature levels would have resulted in less expansion of the material.

Local buckling of the outer tube and the final state of Specimen S2 are shown [Figs. 8(e and f)]. Compared to similar photos from the other two specimens the shape of the local buckling for Specimen S2 was closer to a flat ring as opposed to those of Specimens S3 and S1, which have local buckling rings with relatively rounder edges. This observation provides an example of combined damage (i.e., more severe local buckling) from the seismic and fire loads on the structure. Higher residual drift and impaired moment resistance of the specimen at its end led to a slightly shorter fire resistance time (less than 10 min in difference) in comparison with the other two specimens.

Results from Stub Columns

Fig. 6(d) shows the history of temperature distribution in SC1 and SC2 measured during the fire test. No structural loads were applied to the two stub columns while being tested under fire. Results showed a similar trend compared to the temperature data from the specimen columns. The maximum temperature reached by the outer tube of stub columns is about 100°C less than the similar records for the full-length columns. This minor difference, which is consistent with the observations (mentioned previously) from the recorded temperature data of the first fire test (conducted on Specimen S3), is considered to be due to the lower air temperature at the bottom of the furnace where the short columns were located, as opposed to the upper part of the furnace (thermocouples for the full-length specimens were located close to the top of the columns).

The recorded temperature curves from the thermocouples installed in the concrete and on the surface of the inner tube for SC1 show a smoother trend as opposed to recordings from the specimen columns. The temperature response recorded on the surface of the inner tube for SC2 shows sudden fluctuations similar to what was seen for the main columns.

Results show that the temperature values for all of the three thermocouples installed in SC2 are about 50°C higher than the values for SC1. Since this difference in temperature values is noticeable from the beginning of the test, it is inferred that the main reason for

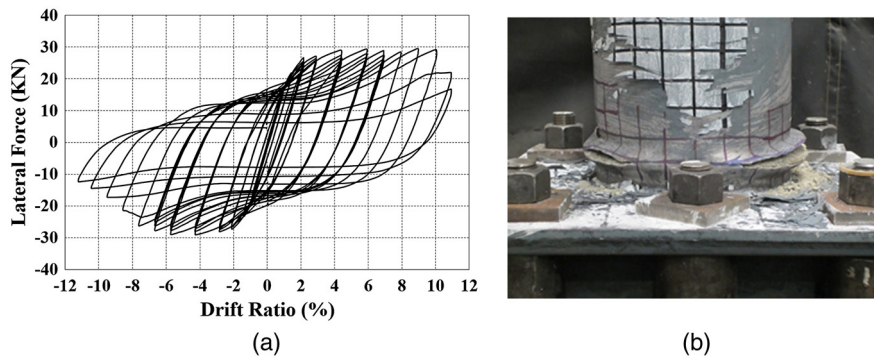


Fig. 9. Post-fire cyclic testing of specimen S3: (a) lateral force versus drift results; (b) fractures at the end of the test

this minor difference is more likely to be related to the different location of the stub columns in the furnace than the number of vent holes used (SC2 had an additional vent hole compared to SC1). This demonstrated that if the minimum required number of vent holes are implemented, the effects of additional vent holes on the overall behavior of CFDST columns will be insignificant. SC1 and SC2 were sitting on the south and north sides of the bottom beam surface, respectively.

Stub columns were also used to study the effects of fire tests on the moisture content of concrete by comparing the measured relative humidity (RH) of the two stub columns tested in fire with that of the third stub column, SC3, which was kept intact in the lab. The RH is the amount of water vapor present in a volume of air at a given temperature to the maximum amount that the air could hold at that temperature, expressed as a percentage. The RH values of the three stub columns were measured based on ASTM F2170 (ASTM 2011). An electronic probe was inserted into holes drilled into the concrete (after running through the steel) to measure the RH values (drilled holes were not located close to the vent holes). Measurements gave post-fire RH values of 29 and 20% for SC1 and SC2, respectively. These values were about half of the RH value of 59% for SC3 which was not fire tested. The effect of the additional vent hole is seen in the difference of RH values for SC1 and SC2.

Post-Fire Cyclic Testing of Specimen S3

Given that Specimen S3 was only subjected to the fire test, a post-fire cyclic loading test was performed in an attempt to investigate the effects of prior fire loading on the flexural behavior of the column under cyclic loading. The column was not loaded axially in this test due to the difficulties caused by its deformed shape. Fig. 9(a) shows the lateral force versus lateral drift ratio curve from the post-fire cyclic testing. The test was continued up to the point that a strength degradation of about 50%, which occurred at a lateral drift ratio of 11%, was recorded in the hysteretic curves and substantial fractures occurred in the lower part of the outer tube on both sides. Fig. 9(b) shows a photo of the fractured column, with cracks over lengths of 280 and 127 mm (11 and 5 in.) on the right and left sides of the column, respectively.

From Fig. 9(a), Specimen S3 retained its ductile behavior after being subjected to fire loading (after cooling down to room temperature). The maximum lateral strength value for the cyclic testing of Specimen S3 was about 29.4 kN (6.6 kips). According to the theoretical P-M interaction diagram for the specimen cross section considered, the absence of axial load in this test (compared to the columns tested previously) would result in a 12% reduction in moment capacity. Therefore, considering that Specimens S1 and S2 would have reached a maximum lateral strength of about 31.1 kN (7 kips) in absence of axial load [i.e., a 12% reduction

of the experimentally recorded value of 35.6 kN (8 kips)], this leaves a 5.7% reduction in maximum lateral strength of Specimen S3 (compared to Specimens S1 and S2) that can be attributed to permanent changes in material strength caused by fire.

Considering the temperature distribution results presented previously, the outer and inner steel tubes along with the concrete core reached maximum temperatures above 800°C (except for the third fire test in which the temperatures were on average 100°C lower), and cooled down to the ambient temperature of about 20°C. In accordance with the Eurocode general rules for structural fire design (CEN 2005), this temperature history is expected to cause a 10% permanent loss in the yield and tensile strength of steel, along with an 85% permanent loss in the compressive strength of the concrete core. Calculation of the moment capacity of the cross section based on these modified strength values shows that the column would have been expected to resist a maximum lateral load of about 28.5 kN (6.4 kips). This calculated strength is in good agreement with the recorded value of 29.4 kN (6.6 kips) from the post-fire cyclic testing of Specimen S3.

Conclusions

Three CFDST columns with different levels of simulated seismic damage (no damage, moderate, and high) were subjected to ASTM E119 (ASTM 2012b) standard fire test. Results indicated that for the particular type of columns built and tested under the mentioned boundary conditions in this paper, differences in the initial conditions based on the simulated seismic damage level had insignificant effects on the fire resistance time of the specimens. The shortest fire resistance time was recorded for the specimen with a residual drift ratio of 3.9% (Specimen S2), which was about 5 min shorter than the 65 min recorded for the undamaged specimen. This suggests that CFDST columns can be particularly effective in resisting the sequential seismic and fire loading. However, since the three fire tests were limited to a specific boundary condition (fixed and semifixed ends) results should not be indiscriminately expanded to other conditions without further experimental and numerical studies (nor should the trends observed be extrapolated to other types of column constructions).

Post-fire cyclic testing of a CFDST column, which was cooled down to the room temperature after being exposed to a 65-min long ASTM E119 (ASTM 2012b) standard fire, showed a permanent loss in lateral strength. The lateral resistance reduction was in good agreement with the expected value calculated based on the modified material properties defined in the Eurocode (CEN 2005) general rules for post-fire situations. Results showed a resilient behavior for CFDST columns in a post-fire cyclic loading scenario,

although the conclusion is based on a single test and needs supplemental studies to generalize these findings.

Acknowledgments

This paper was supported by the MCEER, University at Buffalo. However, any opinions, findings, conclusions, and recommendations presented in this paper are those of the writers and do not necessarily reflect the views of the sponsors.

References

- American Institute of Steel Construction (AISC). (2003). *Design guide 19: Fire resistance of structural steel framing*, Chicago.
- American Institute of Steel Construction (AISC). (2010). *Specification for structural steel buildings*, Chicago.
- Applied Technology Council (ATC). (1992). "Guidelines for cyclic seismic testing of components of steel structures." *ATC-24*, Redwood City, CA.
- ASTM. (2011). "Standard test method for determining relative humidity in concrete floor slabs using in situ probes." *F2170-11*, West Conshohocken, PA.
- ASTM. (2012a). "Standard specification for electric-resistance-welded carbon and alloy steel mechanical tubing." *A513/A513M-12*, West Conshohocken, PA.
- ASTM. (2012b). "Standard test methods for fire tests of building construction and materials." *E119-12a*, West Conshohocken, PA.
- Espinos, A., Romero, M. L., and Hospitaler, A. (2010). "Advanced model for predicting the fire response of concrete filled tubular columns." *J. Constr. Steel Res.*, 66(8–9), 1030–1046.
- European Committee for Standardization (CEN). (2005). *Eurocode 4: Design of composite steel and concrete structures, part 1.2: General rules—Structural fire design*, Brussels, Belgium.
- Fouche, P., and Bruneau, M. (2010). "Non-linear analysis of multi-hazard performance of concrete filled steel tubes bridge piers." *8th Int. Conf. on Short and Medium Span Bridges 2010*, Canadian Society for Civil Engineering (CSCE), West Montréal, QC, Canada.
- Hajjar, J. F. (2000). "Concrete-filled steel tube columns under earthquake loads." *Prog. Struct. Eng. Mater.*, 2(1), 72–81.
- Han, L. H. (2001). "Fire performance of concrete filled steel tubular beam-columns." *J. Constr. Steel Res.*, 57(6), 697–711.
- Han, L. H., Tao, Z., Huang, H., and Zhao, X. L. (2004). "Concrete-filled double skin (SHS outer and CHS inner) steel tubular beam-columns." *Thin Wall Struct.*, 42(9), 1329–1355.
- Han, L. H., and Yang, Y. F. (2005). "Cyclic performance of concrete-filled steel CHS columns under flexural loading." *J. Constr. Steel Res.*, 61(4), 423–452.
- Han, L. H., Zhao, X. L., Yang, Y. F., and Feng, J. B. (2003). "Experimental study and calculation of fire resistance of concrete-filled hollow steel columns." *J. Struct. Eng.*, 10.1061/(ASCE)0733-9445(2003)129:3(346), 346–356.
- Hong, S., and Varma, A. H. (2009). "Analytical modeling of the standard fire behavior of loaded CFT columns." *J. Constr. Steel Res.*, 65(1), 54–69.
- Kodur, V. K. R. (1998). "Performance of high strength concrete-filled steel columns exposed to fire." *Can. J. Civ. Eng.*, 25(6), 975–981.
- Lu, H., Han, L. H., and Zhao, X. L. (2010). "Fire performance of self-consolidating concrete filled double skin steel tubular columns: Experiments." *Fire Saf. J.*, 45(2), 106–115.
- Lu, H., Zhao, X. L., and Han, L. H. (2011). "FE modelling and fire resistance design of concrete filled double skin tubular columns." *J. Constr. Steel Res.*, 67(11), 1733–1748.
- Marson, J., and Bruneau, M. (2004). "Cyclic testing of concrete-filled circular steel bridge piers having encased fixed-based detail." *J. Bridge Eng.*, 10.1061/(ASCE)1084-0702(2004)9:1(14), 14–23.
- Moliner, V., Espinos, A., Romero, M. L., and Hospitaler, A. (2013). "Fire behavior of eccentrically loaded slender high strength concrete-filled tubular columns." *J. Constr. Steel Res.*, 83, 137–146.
- NIST. (1996). "The January 17, 1995 Hyogoken-Nabu (Kobe) earthquake; performance of structures, lifelines, and fire protection systems." *NIST Special Publication 901*, Gaithersburg, MD.
- NOAA. (1972). "A study of earthquake losses in the San Francisco bay area—Data and analysis." *Rep. Prepared for the Office of Emergency Preparedness*, Washington, DC.
- Uenaka, K., Kitoh, H., and Sonada, K. (2008). "Concrete-filled double skin tubular members subjected to bending." *Steel Compos. Struct.*, 8(4), 297–312.
- Yang, Y. F., and Han, L. H. (2008). "Concrete-filled double-skin tubular columns under fire." *Mag. Concrete Res.*, 60(3), 211–222.
- Zhao, X. L., and Grzebieta, R. (2002). "Strength and ductility of concrete filled double skin (SHS inner and SHS outer) tubes." *Thin Wall Struct.*, 40(2), 199–213.